Published OnlineFirst May 11, 2010; DOI: 10.1158/0008-5472.CAN-09-3028

Cancer Research

Inhibition of Histone Deacetylase in Cancer Cells Slows Down Replication Forks, Activates Dormant Origins, and Induces DNA Damage

Chiara Conti, Elisabetta Leo, Gabriel S. Eichler, Olivier Sordet, Melvenia M. Martin, Angela Fan, Mirit I. Aladjem, and Yves Pommier

Abstract

Protein acetylation is a reversible process regulated by histone deacetylases (HDAC) that is often altered in human cancers. Suberoylanilide hydroxamic acid (SAHA) is the first HDAC inhibitor to be approved for clinical use as an anticancer agent. Given that histone acetylation is a key determinant of chromatin structure, we investigated how SAHA may affect DNA replication and integrity to gain deeper insights into the basis for its anticancer activity. Nuclear replication factories were visualized with confocal immunofluorescence microscopy and single-replicon analyses were conducted by genome-wide molecular combing after pulse labeling with two thymidine analogues. We found that pharmacologic concentrations of SAHA induce replication-mediated DNA damage with activation of histone γH2AX. Single DNA molecule analyses indicated slowdown in replication speed along with activation of dormant replication origins in response to SAHA. Similar results were obtained using siRNA-mediated depletion of HDAC3 expression, implicating this HDAC member as a likely target in the SAHA response. Activation of dormant origins was confirmed by molecular analyses of the β-globin locus control region. Our findings demonstrate that SAHA produces profound alterations in DNA replication that cause DNA damage, establishing a critical link between robust chromatin acetylation and DNA replication in human cancer cells. *Cancer Res; 70(11); 4470–80. ©2010 AACR.*

Introduction

Abnormalities in DNA replication are a major cause of genomic instability, a hallmark of cancer cells. It is therefore important to understand the mechanisms regulating DNA replication, chromatin structure, and cell cycle progression. DNA replication must be coupled with the cell cycle to coordinate the activation of thousands of origins with the velocity of replication forks to fully replicate the genome within each cell cycle (1, 2). In metazoans, it is still not clear how origins of replication are selected, and a large number of potential origins remain quiescent. These dormant origins initiate replication when replication forks coming from neighboring origins experience a slowing down or an arrest (3–6). Stalled forks must be stabilized and processed to avoid inappropriate recombination and genomic instability (7, 8), and these processes involve chromatin remodeling and histone modifications (9–11).

The accessibility of origins to the replication proteins is likely to be influenced by chromatin structure and compaction. Acetylation on lysines facilitates an "open" chromatin status by neutralizing the positive charges of lysines on histones (12). It also plays a regulatory role during DNA replication by facilitating both the removal of histones from the DNA template and the reloading of histone on newly replicated DNA (9, 10, 13–18). In addition, deacetylation of newly incorporated histones plays a major role in chromatin maturation (9, 18, 19).

Histone deacetylases (HDACs; also called lysine deacetylases) and histone acetyl transferases are enzymes that ensure the homeostatic levels of histone acetylation. They also act reversibly on many other proteins in human cells. A recent analysis revealed at least 3,600 acetylation sites in 1,750 different human proteins (20). Human cells have 18 zinc-dependent HDACs organized in four classes (21, 22). Class I HDACs are nuclear and consist of HDAC1, HDAC2, HDAC3, and HDAC8, which are orthologs of the *Saccharomyces cerevisiae* Rpd3. Yeast cells lacking Rpd3 display a delay in S-phase progression, as measured by flow cytometry (23). Two-dimensional gel analysis showed that *rpd3Δ* mutants have deregulated timing of origin firing, with late origins being activated early (17, 23, 24). The other HDACs

Authors' Affiliation: Laboratory of Molecular Pharmacology, National Cancer Institute, NIH, Bethesda, Maryland

Note: Supplementary data for this article are available at Cancer Research Online (http://cancerres.aacrjournals.org/).

C. Conti and E. Leo contributed equally to this work.

Current address for C. Conti: Dana-Farber Cancer Institute, Harvard, Cambridge, Massachusetts. Current address for O. Sordet: Institut Claudius Regaud, Institut National de la Sante et de la Recherche Medicale U563, Toulouse, France.

Corresponding Author: Yves Pommier, NIH/National Cancer Institute, 37 Convent Drive, Building 37, Room 5068, Bethesda, MD 20892-4255. Phone: 301-496-5944; Fax: 301-402-0752; E-mail: pommier@nih.gov.

doi: 10.1158/0008-5472.CAN-09-3028

Published OnlineFirst May 11, 2010; DOI: 10.1158/0008-5472.CAN-09-3028

(class IIa, IIb, and IV) are primarily cytoplasmic and shuttle between the nucleus and cytoplasm. In contrast to the aforementioned zinc-dependent HDACs, class III HDACs (the sirtuins) are NAD dependent and are not targeted by the HDAC inhibitors (HDACi). All HDACs are components of large multiprotein complexes (22).

HDACs are important drug targets for cancer and neurodegenerative diseases (Parkinson and Alzheimer syndromes), and there are >60 clinical trials currently under way. Given their broad regulatory role, HDACs are complex targets for cancer therapy. HDACi generally target more than one class of zinc-dependent HDAC, and several pathways are likely to be involved in their anticancer activity (22). Suberoylanilide hydroxamic acid (SAHA; ref. 25) was the first HDACi approved by the Food and Drug Administration. SAHA is a broad-spectrum HDACi targeting both class I and II HDACs. It is marketed as Vorinostat (Zolinza) for the treatment of cutaneous T-cell lymphomas (22). A number of clinical trials are ongoing to explore additional uses for SAHA as an anticancer drug in combination therapies and to evaluate other HDACi (22, 26). Although SAHA is known to induce histone hyperacetylation as early as 4 hours after exposure (27), most studies have focused on the ability of SAHA to induce cell differentiation and apoptosis after long exposures, typically 24 hours or longer (28).

Because of the growing importance of SAHA and HDACi as anticancer therapies (22, 26) and of our interest in DNA replication (1), genomic integrity (29), and molecular pharmacology (30, 31), we investigated the effects of pharmacologic concentrations (32) of SAHA on replication fork progression, replication initiation, and DNA integrity in human cells. We also studied the contribution of HDAC3 to the effects of SAHA on DNA replication.

Materials and Methods

Cell lines

MCF-7 and HCT116 cells were cultured in DMEM and MDA-MB-231 cells in RPMI 1640 (Life Technologies) with 10% FCS (Gemini Bioproducts). Human peripheral lymphocytes from healthy donors were obtained from the NIH Blood Bank and maintained in RPMI 1640 with 10% FCS.

siRNA transfections

siRNA was prepared in 750 μL RPMI 1640 (80 nmol/L final concentration) and mixed with 750 μL RPMI 1640 containing 3 μL Lipofectamine RNAiMAX Reagents (Invitrogen) in a six-well plate. The mixture was incubated for 30 minutes before addition of 10^5 MDA-MB-231 cells in 1.5 mL RPMI 1640 supplemented with 10% FCS for an additional 72 hours.

Western blotting and antibodies

Cell pellets were resuspended in 100 μL lysis buffer [1% SDS, 10 mmol/L Tris (pH 7.4), 40 μL of 25× protease inhibitors (Roche), 10 μL phosphatase inhibitors (Sigma), 1 mL water]. Total cell lysates (10–30 μg) were loaded in 4% to 20% Tris-glycine gel (Invitrogen) and transferred to nitrocellulose membrane with a semidry apparatus overnight at 4 V. Membranes were blocked in 6% milk and 0.2% Tween 20. The γH2AX antibody (Upstate-Millipore) was used at a 1:2,000 dilution, the H3K9ac antibody (Upstate-Millipore) at 1:2,500 dilution, and the thymidylate synthase (TS) antibody (Thermo Scientific) at 1:100 dilution. Antibodies against ribonucleotide reductase (RNR) RR1 and RR2 were from Chemicon International (Upstate-Millipore) and Santa Cruz Biotechnology, respectively. Antibody signals were detected with Super-Signal West Pico Chemiluminescent Substrate (Pierce).

Immunofluorescence microscopy

Cells were grown with 1 mL medium in four-well chamber slides (Nalge-Nunc International), and staining was performed as described (33). γH2AX antibody was used at 1:2,000 dilution followed by anti-mouse Alexa Fluor 488 (Invitrogen) diluted 1:500. Phospho-53BP1-Ser^{1778} was detected with a primary antibody from Cell Signaling diluted 1:400, followed by secondary anti-rabbit Alexa Fluor 568 antibody (Invitrogen).

DNA replication foci were visualized by incorporation of chlorodeoxyuridine (CldU) and iododeoxyuridine (IdU) as described (33). Briefly, cells were pulse labeled with 100 μmol/L IdU and CldU (Sigma), washed with PBS, fixed with cold 70% ethanol, and stored at 4°C. Primary anti-CldU (Accurate Chemical Scientific) and anti–IdU-FITC (BD Pharmingen) antibodies were diluted 1:200, added to the slides, and incubated in a humid environment for 2 hours. Secondary antibodies for CldU and IdU were donkey anti-rat Alexa Fluor 594 and goat anti-mouse Alexa Fluor 488, respectively (Molecular Probes), used at 1:500 dilution. Images were visualized with a Nikon Eclipse TE-300 confocal microscope (33).

COMET assays

Neutral COMET assays were performed (Trevigen) after electrophoresis at 4°C. Tail lengths were measured with Comet IV program, and data were transferred into SigmaPlot 9.0 software to generate the box plot histogram.

Single DNA molecule analyses of replicons

Molecular combing was performed as described (33, 34). Briefly, at the end of the CldU pulse, trypsinized cells were embedded in low-melting agarose plugs. After digestion with β-agarase (New England Biolabs), DNA was combed on silanized surfaces (Microsurfaces, Inc.) and replicons were detected with anti-IdU and anti-CldU antibodies (33). Images were captured with the software Attovision using the epifluorescence microscope Pathway (Becton Dickinson). Signals were measured using ImageJ (open source from National Cancer Institute, NIH) with custom-made modifications.

Replication of nascent strand protocol

Nascent strand protocol was carried out as previously described with few variations (35). Briefly, MCF-7 cells were treated with 1.25 or 10 μmol/L SAHA for an hour before harvesting. After harvesting cells, we followed our published protocol (35). Nascent strands were then analyzed by real-time

Published OnlineFirst May 11, 2010; DOI: 10.1158/0008-5472.CAN-09-3028

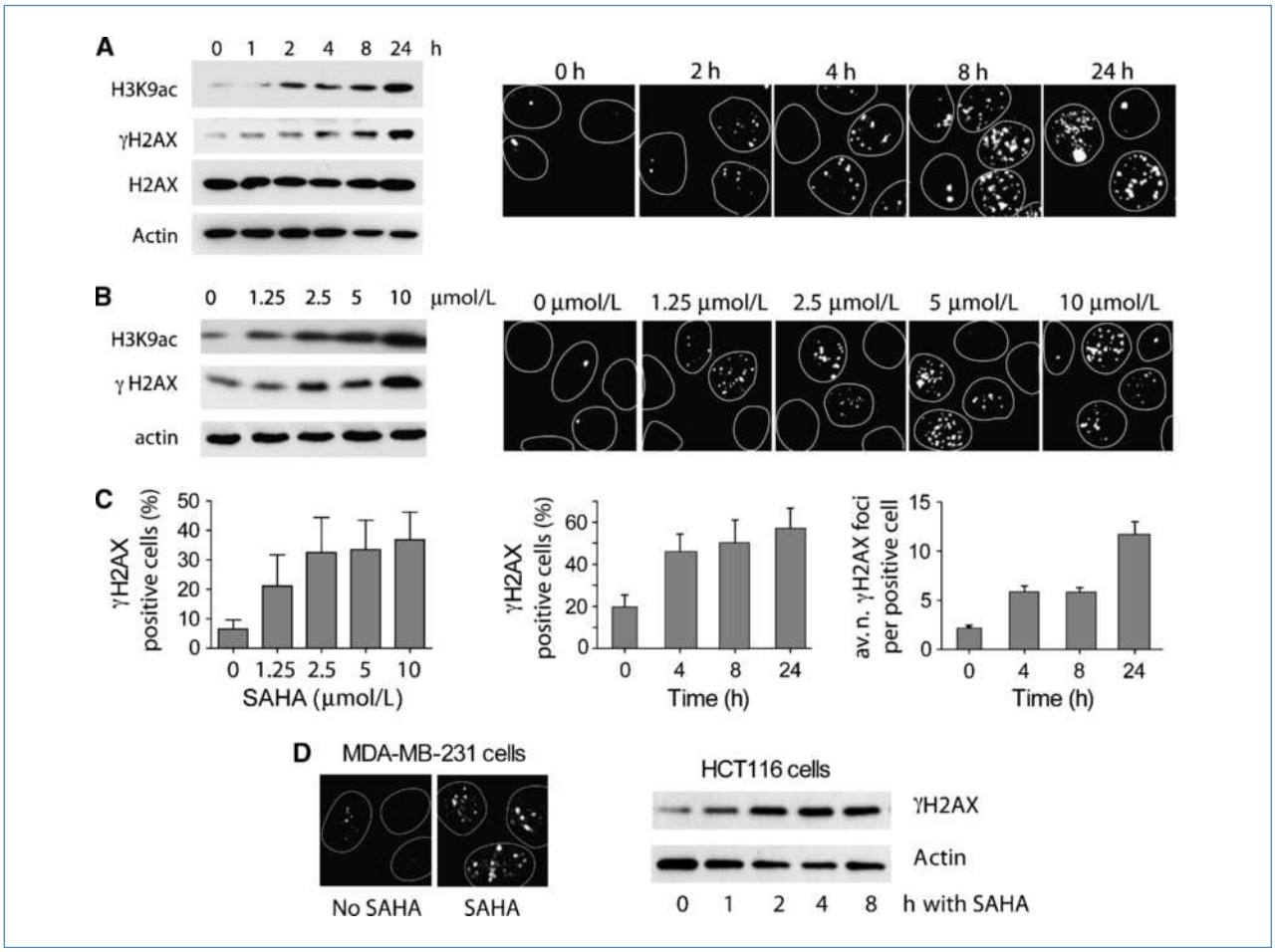

Figure 1. Time- and concentration-dependent induction of γH2AX in response to SAHA. A, breast carcinoma MCF-7 cells were exposed to 1.25 μmol/L SAHA for 1 to 24 h. Left, representative Western blots showing acetylation of histone H3 on Lys^9 (H3K9ac) and γH2AX induction. Total H2AX was examined in parallel. Tubulin was used as a loading control. Right, representative images of γH2AX observed by immunofluorescence microscopy in interphase nuclei. Nuclear outlines are shown. B, MCF-7 cells were treated for 4 h with the indicated SAHA concentrations. Left, concentration-dependent induction of H3K9ac and γH2AX. Actin was used as a loading control. Right, representative images of γH2AX foci observed by immunofluorescence microscopy. Nuclear outlines are shown. C, quantitation of γH2AX induction by SAHA in MCF-7 cells. Left, quantification of γH2AX foci induced by increasing concentrations of SAHA for 4 h. Middle and right, quantification of γH2AX foci induced by 1.5 μmol/L SAHA for the indicated times. Columns, mean of three independent experiments; bars, SD. D, induction of γH2AX by SAHA in breast carcinoma MDA-MB-231 cells (1.25 μmol/L for 4 h; left) and in colon carcinoma HCT116 cells treated with 1.25 μmol/L SAHA for the indicated times (right). Experiments have been repeated at least thrice with consistent results.

PCR (RT-PCR) for initiation activity near the known replication origin [the initiation region (IR)] or at a distal site that usually does not initiate replication [the initiation region (LCR)] on the human β-globin locus.

Results

Short exposure to SAHA induces DNA damage

Because γH2AX (phosphorylated histone H2AX on Ser^{139}) is selectively activated by DNA damage and is a sensitive biomarker (31), we determined whether SAHA induces γH2AX under conditions where it induces hyperacetylation. Exposure of human breast cancer MCF-7 cells to 1.25 μmol/L SAHA revealed hyperacetylation within 2 hours, as shown by the increased acetylation of histone H3 at Lys^9 (H3K9ac; Fig. 1A, left). Increased γH2AX was also detectable after 2-hour treatment, but the signal was more robust and consistent after 4 hours (Fig. 1A, left). To investigate whether the γH2AX induction was dose dependent, MCF-7 cells were treated for 4 hours with increasing SAHA concentrations from 1.25 to 10 μmol/L. On Western blot, H3K9ac increased with increasing SAHA concentration (Fig. 1B, left).

To further show the γH2AX DNA damage response induced by SAHA, we used immunofluorescence microscopy because it is more sensitive than Western blotting, as it can detect an isolated double-strand break (DSB; ref. 31). Figure 1A and B (right) shows that γH2AX was induced in focal pattern, which is typical of cells experiencing DNA damage response (31). The number of γH2AX-positive

Published OnlineFirst May 11, 2010; DOI: 10.1158/0008-5472.CAN-09-3028

cells and the number of γH2AX foci per nucleus increased with increasing the SAHA concentration and exposure time (Fig. 1A–C).

Another breast cancer cell line, MDA-MB-231, which is p53 mutant and triple negative for estrogen receptor, progesterone receptor, and epidermal growth factor receptor 2, also showed γH2AX induction in response to SAHA (Fig. 1D, left). Similarly, we found induction of γH2AX in human colon carcinoma HCT116 cells (Fig. 1D, right), confirming the induction of DNA damage by SAHA in different cancer cell lines.

SAHA can be released from its binding site on HDAC when removed from treated cells, thus allowing deacetylation (36). To further characterize the SAHA-induced DNA damage response, histone acetylation and γH2AX were monitored after drug removal following 4-hour treatments with 1.25 or 10 μmol/L SAHA. Acetylation of H3K9 diminished as early as 20 minutes after SAHA removal and returned back to normal within 1 hour (Supplementary Fig. S1A and B). γH2AX levels also decreased within 1 or 2 hours (Supplementary Fig. S1C). Immunofluorescence analysis showed that the average γH2AX intensity per positive cell decreased rapidly after drug removal, which correlates with Western blotting results. However, γH2AX-positive cells persisted for at least 4 hours (Supplementary Fig. S1D), suggesting that some DNA damage repair requires a long time frame.

γH2AX was initially described as a marker for DNA DSBs (37). However, a growing body of evidence suggests that γH2AX can also appear when the cells experience damages other than DSBs (31). To address whether the SAHA-induced γH2AX foci correspond to DSBs, we looked for colocalization of the γH2AX foci with phosphorylated 53BP1 foci, another marker for DSBs. MCF-7 cells were treated for 4 hours with 10 μmol/L SAHA or 1 μmol/L camptothecin [known to induce replication-associated DSBs (38) and used as positive control]. As for camptothecin, phospho-53BP1 colocalized with the γH2AX foci in SAHA-treated cells (Fig. 2A). To test directly for DSBs, we performed neutral COMET assays, which detect broken DNA. COMET tail length and tail moment increased in response to SAHA (Fig. 2B–D), thus confirming the induction of DSBs.

Replication dependence of SAHA-induced DNA damage

To assess the contribution of DNA replication to SAHA-induced DNA damage, we first tested whether the γH2AX foci colocalized with replication factories (7, 33). Cells were treated with SAHA for 4 hours and pulse labeled with CldU to detect replication factories by immunofluorescence microscopy (33). Eighty percent of the γH2AX foci colocalized with replication factories (labeled with CldU), and ~50% of the replication factories were γH2AX positive in SAHA-treated cells (Fig. 3A).

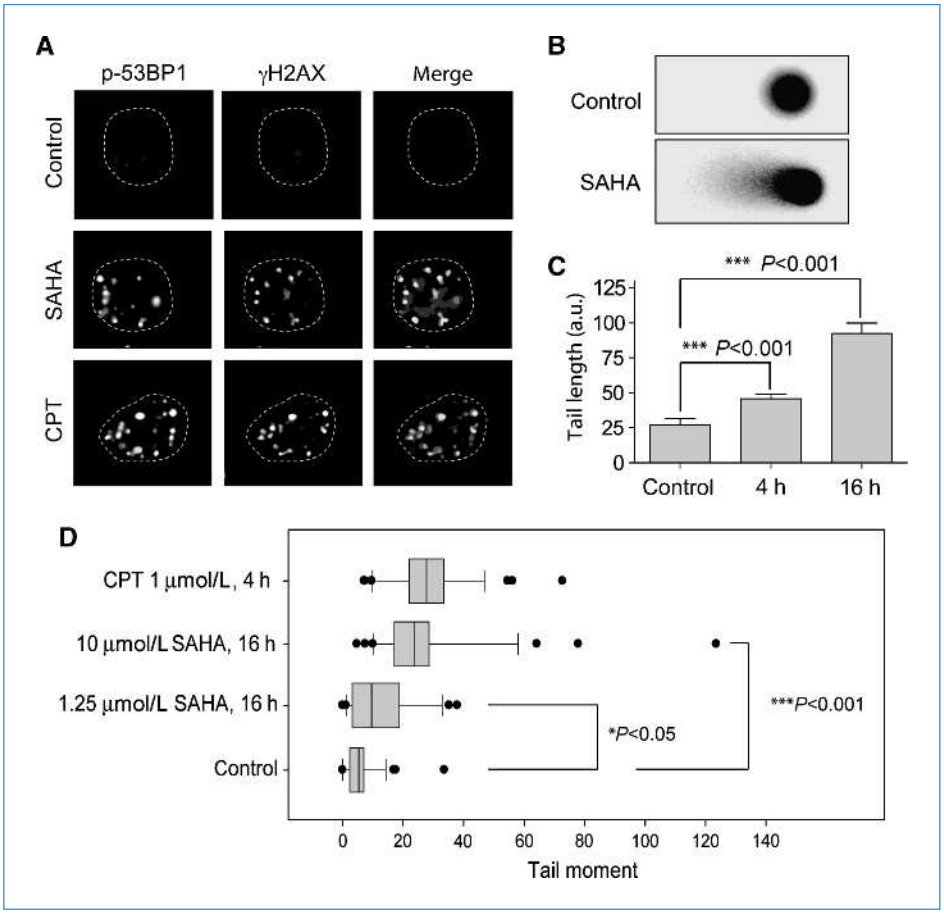

Figure 2. Induction of DNA DSBs by SAHA. A, colocalization of γH2AX foci (middle) with phospho-53BP1 (left) foci in MCF-7 cells treated with SAHA (10 μmol/L) or camptothecin (CPT; 1 μmol/L) for 4 h. Nuclear outlines are shown with dotted lines. B, representative images of COMET tails obtained in an untreated sample and in MCF-7 cells treated with 10 μmol/L SAHA for 16 h. C, quantification of the COMET tail length in cells treated for 4 or 16 h with 10 μmol/L SAHA (see Materials and Methods). a.u., arbitrary unit. The assay was repeated thrice. The graph shows the result of a representative experiment. The statistical significance was calculated with the Mann-Whitney test. D, quantification of the COMET tail moment for samples including at least 35 cells each. In the box plot, the gray area boxes represent the interval where the middle 50% of the data lie and the vertical line in the gray box represents the median. The horizontal bars extending from the boxes encompass the data set within a 95% confidence interval. The dots are outliers.

Published OnlineFirst May 11, 2010; DOI: 10.1158/0008-5472.CAN-09-3028

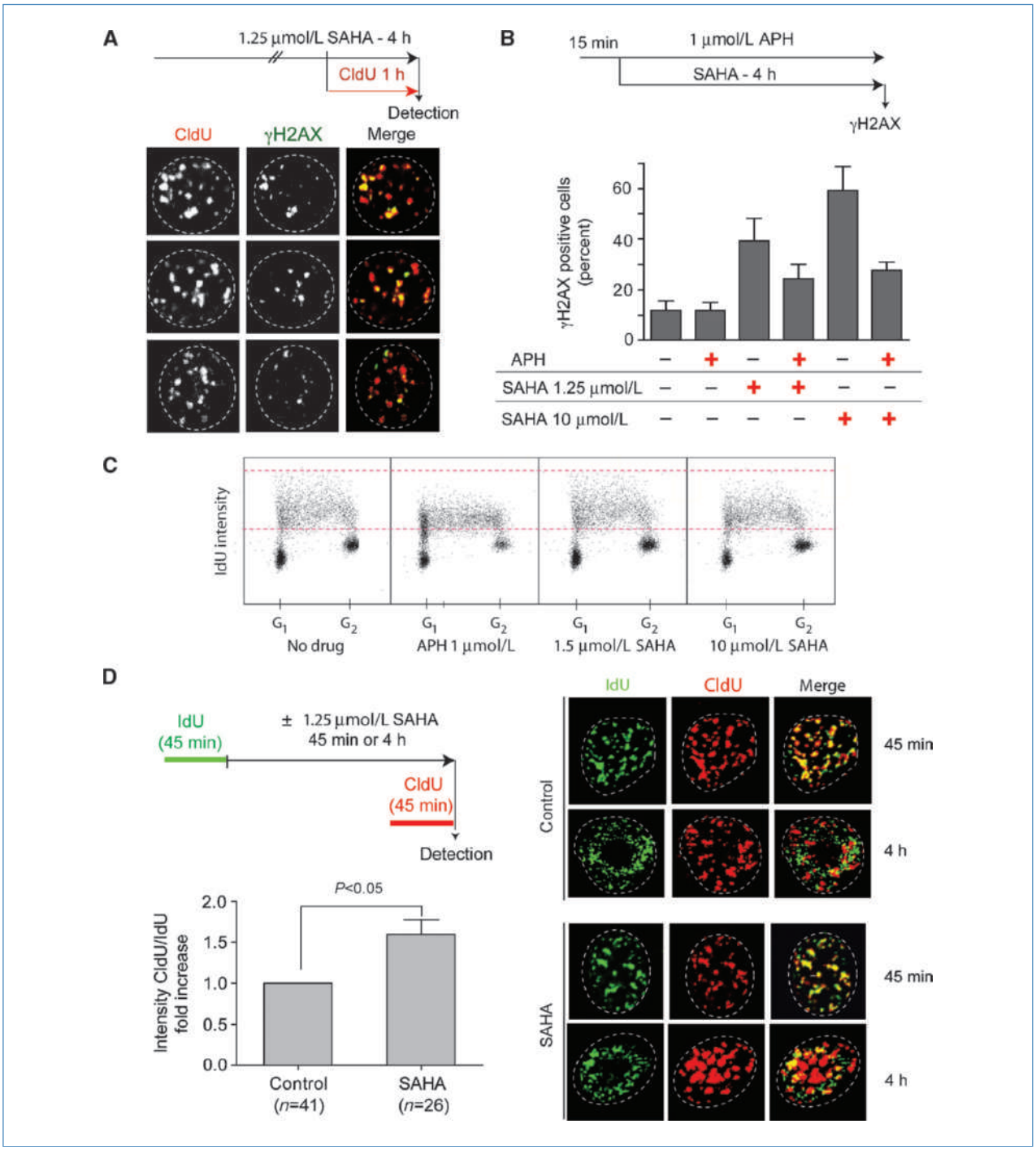

Figure 3. Single-cell analyses of DNA replication–associated γH2AX induction by SAHA. A, MCF-7 cells were treated with 1.25 μmol/L SAHA for 4 h and pulse labeled with CldU during the last hour of treatment to label replication factories (schematized at top; ref. 33). CldU and γH2AX were detected by immunofluorescence in red and green, respectively. Representative cells treated with SAHA show the colocalization of γH2AX with DNA replication factories (CldU). B, MCF-7 cells were pretreated with 1 μmol/L aphidicolin (APH) followed by 4-h coexposure with aphidicolin and SAHA (scheme at the top). Bottom, quantification of the γH2AX response to 1.25 or 10 μmol/L SAHA in the presence or absence of aphidicolin. Columns, mean of at least three independent determinations; bars, SD. C, FACS profile of cells treated for 4 h with aphidicolin or SAHA at the indicated concentrations and pulse labeled with IdU for the last 5 min of the treatment. The horizontal dotted lines show the decreased incorporation of IdU in aphidicolin- and SAHA-treated cells. D, immunofluorescence analyses of DNA replication dynamics in individual cells treated with SAHA. MCF-7 cells were pulse labeled for 45 min with IdU, treated for 4 h or 45 min with SAHA, and pulse labeled with CldU during the last 45 min. IdU and CldU were then detected in green and red, respectively. Representative nuclei from untreated (control) and SAHA-treated cells are shown. Bottom left, quantification of the CldU/IdU intensity ratio. The control data have been normalized to 1. Columns, mean of three independent experiments; bars, SD.

Published OnlineFirst May 11, 2010; DOI: 10.1158/0008-5472.CAN-09-3028

The functional relationship between DNA replication and γH2AX was further examined under conditions where DNA replication was inhibited with aphidicolin (see pulse-labeling experiment in Fig. 3C showing reduction of CldU incorporation and accumulation of cells at the G_1-S boundary in the presence of aphidicolin; ref. 38). Cotreatment with 1 μmol/L aphidicolin reduced the γH2AX signal after 4-hour exposure to SAHA (Fig. 3B) under conditions where aphidicolin by itself did not induce γH2AX foci (7). These results provide further evidence for the induction of replication-associated DNA damage by SAHA.

Because we observed some γH2AX-positive MCF-7 cells that did not stain for replication factories, we assessed γH2AX induction by SAHA in nonreplicating cells. To do so, we treated postmitotic circulating human lymphocytes with SAHA and looked for γH2AX by immunofluorescence microscopy (39). On average, two γH2AX foci per cell were visible after 6-hour treatment with 5 μmol/L SAHA (Supplementary Fig. S2A). Fluorescence-activated cell sorting (FACS) analysis also showed an increase in the percentage of γH2AX-positive cells, which was reduced when cells were treated with the transcription inhibitor flavopiridol (Supplementary Fig. S2B; ref. 39). Together, these results show that SAHA can induce both replication- and transcription-dependent DNA damage. In the remaining part of this study, we chose to focus on the effects of SAHA on DNA replication.

SAHA alters DNA synthesis

Because our data show that SAHA induces DSBs and activates the DNA damage response in replication factories, FACS analyses with pulse labeling were performed to monitor DNA replication in SAHA-treated cells. As before, MCF-7 cells were treated for 4 hours with SAHA but replication was also monitored by pulse labeling with IdU, a thymidine analogue, during the last 5 minutes of the SAHA treatment. FACS analysis with anti-IdU antibodies detected the cells that were replicating during drug treatment. Aphidicolin was used as positive control for replication inhibition (Fig. 3C, second panel from left). The FACS and IdU profiles of SAHA-treated cells showed a small but consistent decrease of the intensity of IdU incorporation. The effect was also observed with 3-minute IdU pulses (data not shown) and was most obvious at 10 μmol/L SAHA (Fig. 3C).

Because histone hyperacetylation (H3K9ac) and DNA damage (γH2AX) responses were apparent at 4 hours, and SAHA only minimally reduced deoxynucleotide triphosphate (dNTP) incorporation under these conditions, we investigated the dynamics of DNA replication by studying the effects of SAHA on replication factories [i.e., the nuclear sites where replication origins fire together (7, 33, 40)]. To visualize those factories, cells were pulse labeled with IdU for 45 minutes. After which, the cells were released in fresh medium with or without SAHA for either 4 hours or 45 minutes. During the last 45 minutes, replication factories were labeled again but this time with CldU (see scheme in Fig. 3D; refs. 30, 33). In untreated cells (control), the same replication factories were labeled with both IdU and CldU when the two pulses immediately followed each other (45 min; yellow dots on the merge images in the right panels in Fig. 3D). On the other hand, each of the two pulses labeled different replication factories when the IdU label was conducted 4 hours before the CldU label because the replication factories labeled during the first pulse had completed their replication at the time of the second pulse. Figure 3D (right; 4-h time points) shows that SAHA-treated cells show no detectable inhibition in the activation of new replication factories. However, we noticed a consistent increase in the intensity of the second pulse and the presence of yellow signals in the cells treated with SAHA for 4 hours (Fig. 3D), which suggested that SAHA might affect replication initiation and fork velocity (see below).

SAHA reduces fork velocity

To test the effects of SAHA on replication fork velocity and origin firing, we used a single DNA molecule approach based on DNA combing (2, 4, 30, 41, 42). Asynchronous MCF-7 cells were treated with 1.5 or 10 μmol/L SAHA for 4 hours and pulsed with IdU during the last 20 minutes of the treatment. After drug removal, cells were washed and pulsed for 20 minutes with fresh medium containing CldU (Fig. 4A). After combing the genomic DNA, newly replicated regions were detected with specific fluorescent antibodies against IdU and CldU. Figure 4B shows typical signals for three different replicons. The replication signals were then measured, and fork velocity was calculated for the signals that had similar length for the IdU and CldU signals (30).

Significant shortening of both the IdU- and CldU-labeled tracks was observed in the SAHA-treated samples compared with untreated cells. The median velocity in MCF-7 cells went from ~0.8 kb/min in control cells to 0.54 and 0.4 kb/min in cells treated with 1.5 and 10 μmol/L SAHA, respectively (Fig. 4B). These results show that SAHA reduces replication fork velocity.

Because previous studies showed decreased TS expression after prolonged exposure to high doses of trichostatin A and SAHA (43), and reduction fork velocity on inhibition of RNR (4), we looked at the levels of TS and RNR on exposure of MCF-7 cells to SAHA (Fig. 4C). TS and the RNR subunits RR1 and RR2 remained relatively unaffected by SAHA during the 4-hour exposure conditions used to study replication fork velocity. These results are consistent with our prior FACS analysis, showing only small reduction of IdU incorporation in MCF-7 cells treated with SAHA under similar conditions (see Fig. 3C). Therefore, the reduction in fork progression observed by molecular combing after 4-hour exposure to SAHA is not due to reduced dNTP synthesis but rather to effects of SAHA on chromatin.

HDAC3 downregulation also reduces replication fork velocity

Because SAHA is a pan-HDACi with multiple protein targets (22), we compared the effects of SAHA with those of histone hyperacetylation by silencing HDAC3 (Fig. 5A), which has recently been shown to be involved in DNA damage control and cell cycle progression (44). IdU incorporation

Published OnlineFirst May 11, 2010; DOI: 10.1158/0008-5472.CAN-09-3028

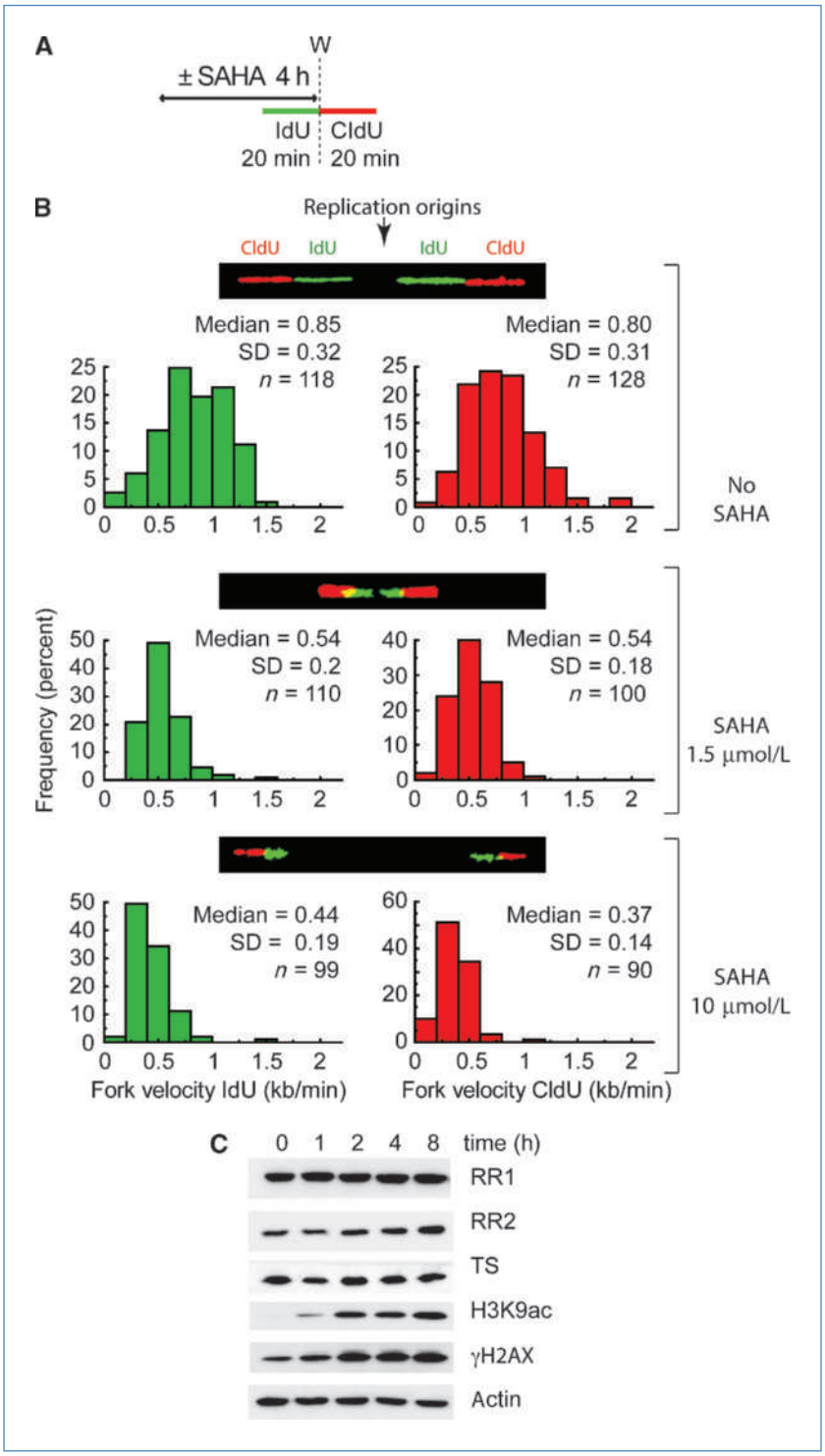

Figure 4. Reduction of replication fork velocity by SAHA. A, cell treatment protocol. MCF-7 cells were treated with 1.5 or 10 µmol/L SAHA for 4 h. The IdU pulse was performed in the last 20 min of treatment. After wash, cells were further incubated for 20 min with CldU. B, representative image and fork velocity analysis on individual combed molecules from untreated cells (top) and cells treated with 1.5 µmol/L (middle) or 10 µmol/L SAHA (bottom). Fork velocity was measured during the IdU (green) and CldU (red) pulses separately. *n*, number of signals scored. For each treatment, at least three independent combing experiments were performed, showing consistent results. C, Western blotting analyses show no detectable effect of SAHA on RNR large and small subunits (RR1 and RR2, respectively) and TS after exposure to 10 µmol/L SAHA for the indicated times. Histone hyperacetylation (H3K9ac) and γH2AX induced by SAHA are also shown at the same time points.

and replication fork velocity were measured in cells transfected for 72 hours with siRNA targeting HDAC3 or with a negative siRNA. FACS analysis showed no detectable effect of HDAC3 silencing on the percentage of cells in S-phase cells and dNTP incorporation (Fig. 5B), which is consistent with the small effects of SAHA on dNTP incorporation and cell cycle (see Fig. 3C). On the other hand, fork velocity was significantly reduced by HDAC3 siRNA (0.8 kb/min) compared with untreated controls (1.3 kb/min; Fig. 5C), which is also consistent with the reduction of fork velocity in response to SAHA (see Fig. 4). These results implicate HDAC3 in the regulation of fork velocity and suggest that HDAC3 is

Published OnlineFirst May 11, 2010; DOI: 10.1158/0008-5472.CAN-09-3028

one of the targets of SAHA with respect to replication fork slow down.

SAHA treatment and HDAC3 depletion both activate dormant origins of replication

Interorigin distance is generally positively correlated with fork velocity (2, 4, 30). When the distance between two neighboring origins increases, the speed of the two forks emanating from those origins also increases. Conversely, as fork velocity decreases, the distance between origins tends to be shorter (2, 4, 30, 45).

Interorigin distances were determined by molecular combing (Fig. 6A and B; ref. 30). Figure 6B shows reduction of the average interorigin distance in cells treated with SAHA compared with untreated cells, indicating that replication origins that do not normally initiate replication in untreated cells are activated in response to SAHA. siRNA-mediated depletion of HDAC3 also showed decreased interorigin distance (Supplementary Fig. S3), confirming the induction of new origins in response to hyperacetylation.

To test the possibility that the increased frequency of initiation corresponded to the activation of dormant origins, we measured replication initiation in the well-characterized human β-globin locus by PCR-based quantification of nascent strand DNA (1, 35). The human β-globin locus contains an active origin of replication (IR) encompassing two replicators: Rep-P and Rep-I (Fig. 6C; ref. 1). Nearby, the LCR is a silent region that does not contain active origins and is replicated passively by the forks traveling from IR. Comparison of the replication activity in the Rep-P and LCR region in untreated and SAHA-treated cells was performed by measuring the abundance of short, nascent DNA strands by RT-PCR (46). Figure 6D shows an increased abundance of nascent strands at both the β-globin Rep-P and LCR loci in SAHA-treated cells. Therefore, the open chromatin status induced by SAHA seems to facilitate the activation of dormant replication origins (such as the LCR locus).

Discussion

Here, we show that SAHA induces replication-associated DNA damage within 4 hours of exposure, as shown by the appearance of γH2AX and phospho-53BP1 foci colocalizing with replication foci, as well as by the appearance of

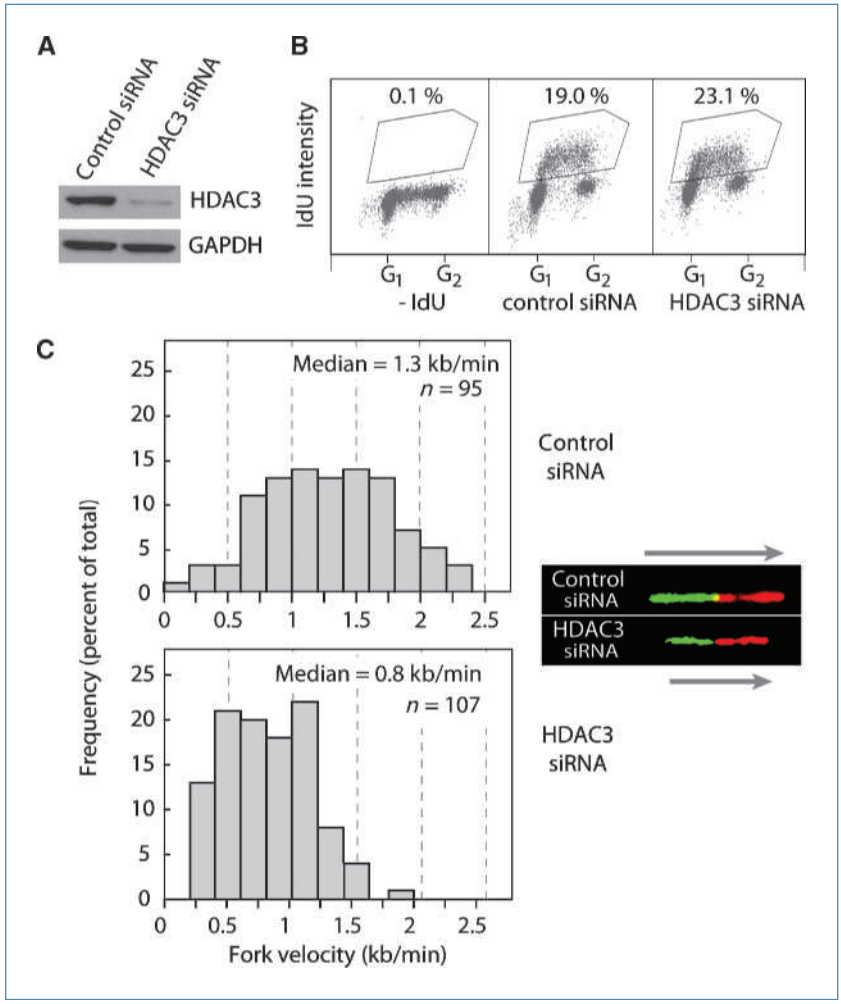

Figure 5. Reduction of replication fork velocity by HDAC3 downregulation. A, Western blotting showing the downregulation of HDAC3 by siRNA in MDA-MB-231 cells. B, FACS analysis of cells transfected for 3 d with a control or HDAC3 siRNA. C, fork velocity measured in cells treated with a control siRNA (top) and the HDAC3 siRNA (bottom). The median values of measured fork speeds are indicated for the two samples. Similar results were obtained in two independent transfection experiments. Representative images are shown at the right.

Published OnlineFirst May 11, 2010; DOI: 10.1158/0008-5472.CAN-09-3028

COMET-positive cells indicative of DSBs. Those effects of SAHA are induced at therapeutically relevant concentrations, as oral administrations result in plasma concentrations between 1 and 2 μmol/L for ~4 hours (32). The DSBs induced by SAHA are detectable within 4 hours of drug exposure and are not the consequence of apoptosis, which is generally observed at least 1 day after exposure to SAHA (22). In addition, the SAHA-induced γH2AX response was characterized by well-defined nuclear foci within replication factories, whereas the γH2AX apoptotic signal does not form foci but rather an intense diffuse peripheral staining of the nuclei, which is referred to as the "apoptotic ring" (47, 48). Moreover, under our experimental conditions (4-h treatment), we did not detect other common signs of apoptosis, such as poly(ADP-ribose) polymerase cleavage, the appearance of stress vesicles or detachment of the cells, nor change in the sub-G_1 area in the FACS cell cycle profiles (even at 24 h after SAHA treatment; Supplementary Fig. S4).

DNA replication–dependent damage occurs when replication forks are blocked and not efficiently stabilized and repaired. Fork arrests have been extensively studied with different agents, such as hydroxyurea that inhibits RNR and blocks replication by depriving DNA polymerase of new dNTPs (4), methyl methanesulfonate that reduces fork progression and origin firing by alkylating DNA (49), aphidicolin that directly inhibits replicative DNA polymerases (4, 7, 11), and camptothecins that induce fork arrest by trapping topoisomerase I and generating replication-associated DSBs with polymerase runoff (33, 38). Those agents, despite their different mechanisms of action, all inhibit DNA replication and induce γH2AX (31). Typically, cells treated with the above replication inhibitors show an enrichment of cells arrested in S phase and inhibition of thymidine incorporation. By contrast, SAHA induces γH2AX without detectable alteration in cell cycle progression, without significant reduction of dNTP incorporation, and without alteration of TS or RNR suggesting lack of checkpoint response (33). Thus, SAHA-induced DNA replication damage is likely the consequence of chromatin hyperacetylation, which in turn interferes with replication initiation and fork progression.

The similarities between the effects of SAHA and HDAC3 silencing by siRNA indicate the relevance of HDAC3 for the cellular effects of SAHA. Our results are consistent with a recent study (44) showing the induction of S-phase–dependent and replication-dependent γH2AX induction and DNA damage in HDAC3$^{-/-}$ murine embryo fibroblasts. In that study (44), SAHA was also shown to activate γH2AX at 24 hours. Our study extends those findings by showing that γH2AX activation takes place within 4 hours of SAHA exposure and is unrelated to apoptosis. We also performed the first single-molecule analyses of DNA replication in HDAC3-downregulated cells and show that HDAC3 downregulation reduces replication velocity and increases origin firing.

Histone acetylation-deacetylation is a dynamic and reversible process that enables chromatin to adapt to DNA replication and transcription. Histone acetylation opens up chromatin by neutralizing the positive charges of lysines and by promoting the binding of bromodomain-containing proteins; both of which enable the loading of DNA processing

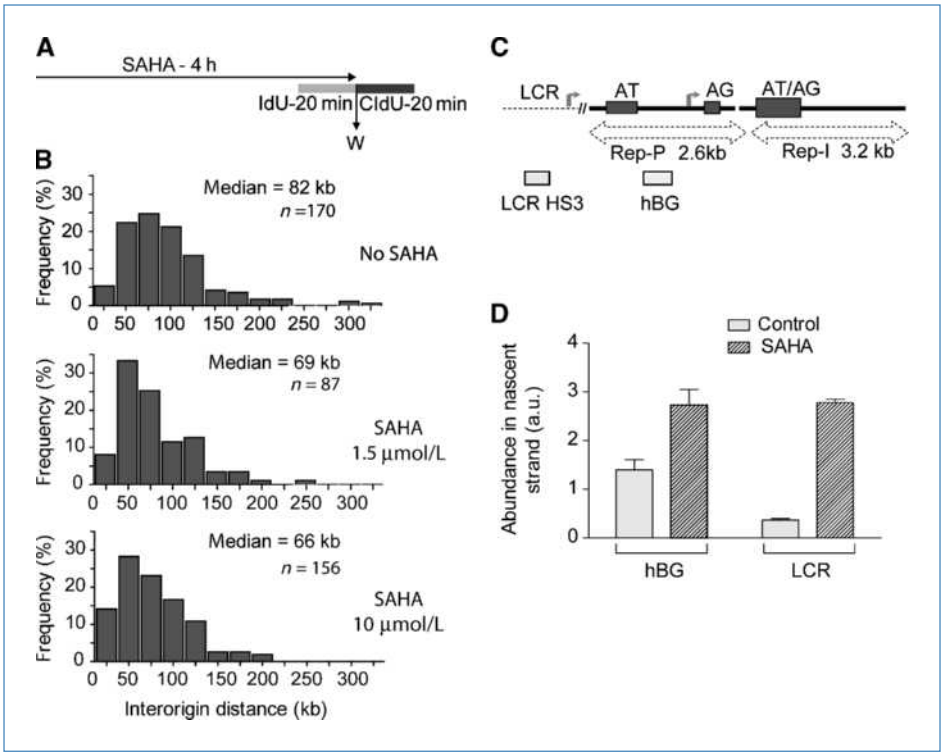

Figure 6. Dormant origins of replication are activated and average interorigin distance is reduced after SAHA treatment. A, MCF-7 cells were treated with 1.5 or 10 μmol/L SAHA for 4 h, and replication forks were analyzed using a dual pulse with IdU and CldU. B, interorigin distance measured on individual molecules from untreated cells (No SAHA) and cells treated with 1.5 and 10 μmol/L SAHA. C, schematic representation of the human β-globin region (LCR) and position of the primers used for the RT-PCR. D, origin activity analyzed in the LCR and human β-globin replicator (hBG) by RT-PCR on nascent strand DNA. Bars, SD.

Published OnlineFirst May 11, 2010; DOI: 10.1158/0008-5472.CAN-09-3028

enzymes. Hyperacetylation facilitates both the removal of histones from the DNA template and the reloading of histone on newly replicated DNA (9, 10, 13–18). Deacetylation of newly incorporated histones also plays a major role in chromatin maturation (9, 18, 19). A recent study shows that a large number of chromatin proteins are acetylated (20). Histones represent only a small fraction of those proteins. Among the chromatin proteins relevant to the present study, Choudhary and coworkers (20) found 52 replication proteins acetylated on 98 sites (including the replication helicases MCM2-6, DNA polymerase, Geminin, Timeless, and Claspin), 26 chromatin remodeling proteins acetylated on 46 sites (including SWI/SNF, NURD, INO80, and NURF), 46 DNA/RNA helicases acetylated on 105 sites, and 132 cell cycle proteins acetylated on 243 sites. Thus, it is likely that the replication defects induced by HDAC3 knockdown and SAHA result from targeting a broad range of chromatin-associated protein complexes.

Fork velocity and interorigin distance are linearly correlated (2, 4), and it has generally been proposed that velocity regulates firing. Indeed, in the case of dNTP depletion and DNA polymerase and topoisomerase I inhibition, reduction of fork velocity is associated with activation of dormant origins (4, 33, 45). Because SAHA alters replication without affecting RNR and TS levels, its effects on fork velocity are likely to be due to chromatin changes rather than by alteration of the dNTP pools. Accordingly, the induction of DSBs and γH2AX foci in replication factories by SAHA suggests that SAHA induces DNA damage that arrests replication forks. It is, however, not excluded that histone hyperacetylation by SAHA can activate dormant origins by facilitating chromatin opening and hyperacetylation of replication complexes (20), which could increase the risk of replication fork encounters, leading to their collapse and thereby reduced fork progression.

From a clinical viewpoint, our study shows that DNA damage can take place in response to SAHA and that such DNA damage needs to be considered for the clinical use and future development of HDAC inhibitors. γH2AX could be used as a convenient pharmacodynamic biomarker for HDAC inhibitors (31).

Disclosure of Potential Conflicts of Interest

No potential conflicts of interest were disclosed.

Grant Support

NIH Intramural Program, Center for Cancer Research, National Cancer Institute, NIH grants Z01 BC 006150-19LMP and 1Z01BC010411-09. E. Leo was partially supported by the Bogue Fellowship (University College London).

The costs of publication of this article were defrayed in part by the payment of page charges. This article must therefore be hereby marked *advertisement* in accordance with 18 U.S.C. Section 1734 solely to indicate this fact.

Received 08/14/2009; revised 03/01/2010; accepted 03/16/2010; published OnlineFirst 05/11/2010.

References

1. Aladjem MI. Replication in context: dynamic regulation of DNA replication patterns in metazoans. Nat Rev Genet 2007;8:588–600.
2. Conti C, Sacca B, Herrick J, Lalou C, Pommier Y, Bensimon A. Replication fork velocities at adjacent replication origins are coordinately modified during DNA replication in human cells. Mol Biol Cell 2007;18:3059–67.
3. Santocanale C, Sharma K, Diffley JF. Activation of dormant origins of DNA replication in budding yeast. Genes Dev 1999;13:2360–4.
4. Anglana M, Apiou F, Bensimon A, Debatisse M. Dynamics of DNA replication in mammalian somatic cells: nucleotide pool modulates origin choice and interorigin spacing. Cell 2003;114:385–94.
5. Ge XQ, Jackson DA, Blow JJ. Dormant origins licensed by excess Mcm2-7 are required for human cells to survive replicative stress. Genes Dev 2007;21:3331–41.
6. Ibarra A, Schwob E, Mendez J. Excess MCM proteins protect human cells from replicative stress by licensing backup origins of replication. Proc Natl Acad Sci U S A 2008;105:8956–61.
7. Shimura T, Torres MJ, Martin MM, et al. Bloom's syndrome helicase and Mus81 are required to induce transient double-strand DNA breaks in response to DNA replication stress. J Mol Biol 2008;375:1152–64.
8. Aguilera A, Gomez-Gonzalez B. Genome instability: a mechanistic view of its causes and consequences. Nat Rev Genet 2008;9:204–17.
9. Groth A. Replicating chromatin: a tale of histones. Biochem Cell Biol 2009;87:51–63.
10. Groth A, Rocha W, Verreault A, Almouzni G. Chromatin challenges during DNA replication and repair. Cell 2007;128:721–33.
11. Shimura T, Martin MM, Torres MJ, et al. DNA-PK is involved in repairing a transient surge of DNA breaks induced by deceleration of DNA replication. J Mol Biol 2007;367:665–80.
12. Kelly WK, Marks PA. Drug insight: histone deacetylase inhibitors-development of the new targeted anticancer agent suberoylanilide hydroxamic acid. Nat Clin Pract Oncol 2005;2:150–7.
13. Li Q, Zhou H, Wurtele H, et al. Acetylation of histone H3 lysine 56 regulates replication-coupled nucleosome assembly. Cell 2008;134:244–55.
14. Jorgensen HF, Azuara V, Amoils S, et al. The impact of chromatin modifiers on the timing of locus replication in mouse embryonic stem cells. Genome Biol 2007;8:R169.
15. Han J, Zhou H, Horazdovsky B, Zhang K, Xu RM, Zhang Z. Rtt109 acetylates histone H3 lysine 56 and functions in DNA replication. Science 2007;315:653–5.
16. Aggarwal BD, Calvi BR. Chromatin regulates origin activity in *Drosophila* follicle cells. Nature 2004;430:372–6.
17. Knott SR, Viggiani CJ, Tavare S, Aparicio OM. Genome-wide replication profiles indicate an expansive role for Rpd3L in regulating replication initiation timing or efficiency, and reveal genomic loci of Rpd3 function in *Saccharomyces cerevisiae*. Genes Dev 2009;23:1077–90.
18. Kohn KW, Aladjem MI, Weinstein JN, Pommier Y. Chromatin challenges during DNA replication: a systems representation. Mol Biol Cell 2008;19:1–7.
19. Annunziato AT, Seale RL. Chromatin replication, reconstitution and assembly. Mol Cell Biochem 1983;55:99–112.
20. Choudhary C, Kumar C, Gnad F, et al. Lysine acetylation targets protein complexes and co-regulates major cellular functions. Science 2009;325:834–40.
21. Yang XJ, Seto E. The Rpd3/Hda1 family of lysine deacetylases: from bacteria and yeast to mice and men. Nat Rev Mol Cell Biol 2008;9:206–18.
22. Marks PA, Xu WS. Histone deacetylase inhibitors: potential in cancer therapy. J Cell Biochem 2009;107:600–8.
23. Vogelauer M, Rubbi L, Lucas I, Brewer BJ, Grunstein M. Histone acetylation regulates the time of replication origin firing. Mol Cell 2002;10:1223–33.
24. Aparicio JG, Viggiani CJ, Gibson DG, Aparicio OM. The Rpd3-Sin3 histone deacetylase regulates replication timing and enables intra-S

Published OnlineFirst May 11, 2010; DOI: 10.1158/0008-5472.CAN-09-3028

origin control in *Saccharomyces cerevisiae*. Mol Cell Biol 2004;24:4769–80.
25. Marks PA, Breslow R. Dimethyl sulfoxide to vorinostat: development of this histone deacetylase inhibitor as an anticancer drug. Nat Biotechnol 2007;25:84–90.
26. Prince HM, Bishton MJ, Harrison SJ. Clinical studies of histone deacetylase inhibitors. Clin Cancer Res 2009;15:3958–69.
27. Munster PN, Troso-Sandoval T, Rosen N, Rifkind R, Marks PA, Richon VM. The histone deacetylase inhibitor suberoylanilide hydroxamic acid induces differentiation of human breast cancer cells. Cancer Res 2001;61:8492–7.
28. Munshi A, Tanaka T, Hobbs ML, Tucker SL, Richon VM, Meyn RE. Vorinostat, a histone deacetylase inhibitor, enhances the response of human tumor cells to ionizing radiation through prolongation of γ-H2AX foci. Mol Cancer Ther 2006;5:1967–74.
29. Tuduri S, Crabbe L, Conti C, et al. Topoisomerase I suppresses genomic instability by preventing interference between replication and transcription. Nat Cell Biol 2009;11:1315–24.
30. Conti C, Seiler J, Pommier Y. The mammalian DNA replication elongation checkpoint: implication of Chk1 and relationship with origin firing as determined by single DNA molecule and single cell analyses. Cell Cycle 2007;6:2760–7.
31. Bonner WM, Redon CE, Dickey JS, et al. γH2AX and cancer. Nat Rev Cancer 2008;8:957–67.
32. Kelly WK, O'Connor OA, Krug LM, et al. Phase I study of an oral histone deacetylase inhibitor, suberoylanilide hydroxamic acid, in patients with advanced cancer. J Clin Oncol 2005;23:3923–31.
33. Seiler JA, Conti C, Syed A, Aladjem MI, Pommier Y. The intra-S-phase checkpoint affects both DNA replication initiation and elongation: single-cell and -DNA fiber analyses. Mol Cell Biol 2007;27:5806–18.
34. Conti C, Caburet S, Schurra C, Bensimon A. Molecular combing. Curr Protoc Cytom 2001. Chapter 8: Unit 8.10.
35. Wang L, Lin CM, Brooks S, Cimbora D, Groudine M, Aladjem MI. The human β-globin replication initiation region consists of two modular independent replicators. Mol Cell Biol 2004;24:3373–86.
36. Finnin MS, Donigian JR, Cohen A, et al. Structures of a histone deacetylase homologue bound to the TSA and SAHA inhibitors. Nature 1999;401:188–93.
37. Rogakou EP, Pilch DR, Orr AH, Ivanova VS, Bonner WM. DNA double-stranded breaks induce histone H2AX phosphorylation on serine 139. J Biol Chem 1998;273:5858–68.
38. Furuta T, Takemura H, Liao ZY, et al. Phosphorylation of histone H2AX and activation of Mre11, Rad50, and Nbs1 in response to replication-dependent DNA double-strand breaks induced by mammalian DNA topoisomerase I cleavage complexes. J Biol Chem 2003;278:20303–12.
39. Sordet O, Redon C, Guirouilh-Barbat J, et al. Ataxia telangiectasia mutated activation of transcription- and topoisomerase I-induced DNA double-strand breaks. EMBO Rep 2009;10:87–93.
40. Leonhardt H, Rahn HP, Weinzierl P, et al. Dynamics of DNA replication factories in living cells. J Cell Biol 2000;149:271–80.
41. Goldar A, Labit H, Marheineke K, Hyrien O. A dynamic stochastic model for DNA replication initiation in early embryos. PLoS One 2008;3:e2919.
42. Norio P, Kosiyatrakul S, Yang Q, et al. Progressive activation of DNA replication initiation in large domains of the immunoglobulin heavy chain locus during B cell development. Mol Cell 2005;20:575–87.
43. Lee JH, Park JH, Jung Y, et al. Histone deacetylase inhibitor enhances 5-fluorouracil cytotoxicity by down-regulating thymidylate synthase in human cancer cells. Mol Cancer Ther 2006;5:3085–95.
44. Bhaskara S, Chyla BJ, Amann JM, et al. Deletion of histone deacetylase 3 reveals critical roles in S phase progression and DNA damage control. Mol Cell 2008;30:61–72.
45. Courbet S, Gay S, Arnoult N, et al. Replication fork movement sets chromatin loop size and origin choice in mammalian cells. Nature 2008;455:557–60.
46. Aladjem MI. The mammalian β globin origin of DNA replication. Front Biosci 2004;9:2540–7.
47. Solier S, Sordet O, Kohn KW, Pommier Y. Death receptor-induced activation of the Chk2- and histone H2AX-associated DNA damage response pathways. Mol Cell Biol 2009;29:68–82.
48. Solier S, Pommier Y. The apoptotic ring: a novel entity with phosphorylated histones H2AX and H2B and activated DNA damage response kinases. Cell Cycle 2009;8:1853–9.
49. Merrick CJ, Jackson D, Diffley JF. Visualization of altered replication dynamics after DNA damage in human cells. J Biol Chem 2004;279:20067–75.

AACR American Association for Cancer Research

Cancer Research

The Journal of Cancer Research (1916–1930) | The American Journal of Cancer (1931–1940)

Inhibition of Histone Deacetylase in Cancer Cells Slows Down Replication Forks, Activates Dormant Origins, and Induces DNA Damage

Chiara Conti, Elisabetta Leo, Gabriel S. Eichler, et al.

Cancer Res 2010;70:4470-4480. Published OnlineFirst May 11, 2010.